Radiation reaction effects on ion acceleration in laser foil interaction

Min Chen, Alexander Pukhov, Tong-Pu Yu
Institut für Theoretische Physik I, Heinrich-Heine-Universität Düsseldorf, 40225 Düsseldorf, Germany

Zheng-Ming Sheng
Department of Physics, Shanghai Jiao Tong University, Shanghai 200240, China
and Beijing National Laboratory for Condensed Matter Physics, Institute of Physics, Beijing 100080, China

Radiation reaction effects on ion acceleration in laser foil interaction are investigated via analytical modeling and multi-dimensional particle-in-cell simulations. We find the radiation effects are important in the area where some electrons move backwards due to static charge separation field at the laser intensity of 10^{22} W/cm^2. Radiation reaction tends to impede these backwards motion. In the optical transparency region ion acceleration is enhanced when the radiation effects are considered.

PACS numbers: 41.75.Jv, 52.38-r, 52.38.Kd

INTRODUCTION

Along with the fast development of laser technology, the power intensity which is inaccessible one decade before becomes reality. The focused laser intensity of 10^{22} W/cm^2 is available today. The new generation of laser system such as ELI is under construction. Focused intensity of 10^{25} W/cm^2 is just forward [1]. By use of such intense laser power, plenty of physical problems can be studied and amount of applications are waiting for discovering. Among them particle acceleration presently and will still attract extensive attentions. Electron acceleration by laser plasma accelerator is aimed to TeV [2], ion acceleration also towards to stable, high and mono-energetic beam [3]. Besides ultrahigh power laser system, plasma mirror technology also makes the high contrast clean pulse possible [4], which makes ultrathin target (∼nm thickness) now applicable for ion acceleration [5]. Unlike the target normal sheath field acceleration (TNSA) [6], radiation pressure dominated ion acceleration (RPA) can have a much longer acceleration distance [7]. Simulation results show ions can get GeV energy when a 20fs long laser pulse with 10^{22} W/cm^2 intensity is used [8]. Besides the two mentioned ion acceleration mechanisms, recently ion acceleration in the optical transparency region named the "laser breakout afterburner" (BOA) [9] has also been studied. It demonstrates that ions can get continuously acceleration even the laser pulse transmits through the ultrathin foil, which also gives a possible way to get high energy ion beams.

As is well known, high energy particles when suffering acceleration self-radiation is concomitant. Radiation reaction effects should be considered when the radiation damping force is comparable to the external one. For the above mentioned processes for particle acceleration, electrons are always endured intensive acceleration. When the laser intensity increases further, the radiation reactions cannot be neglected. Naumova *et al.* have studied the radiation reaction effect on the laser hole boring process and point out it plays a positive role as it allows one to maintain the electron thermal energy on a relatively low level and prevents the electron backward motion through the pulse [10].

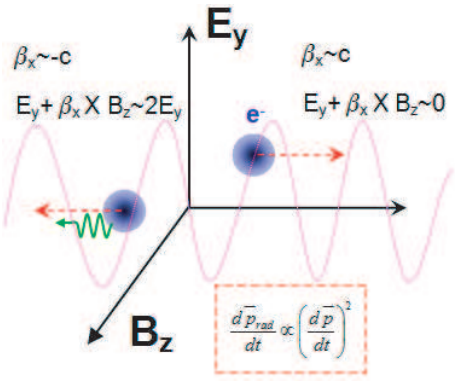

Figure 1: (color online) Sketch map of laser electron interaction. Here a linearly polarized laser pulse is used.

In the present paper, we study their effects on ion acceleration. As a primary result, we find the radiation mainly comes from the electrons moving backwards in the laser pulse and the radiation damping impedes this kind of backward motion, which can reduce the particles' volume in the phase space and improve the ion acceleration energy and quality.

RADIATION AND ITS EFFECT

Before showing the effect of radiation damping, we first check the threshold of the laser intensity for the important radiation reaction effects from existed fundamental formulae. For an electron with velocity $v\sim c$, one can get the radiation power $P(t)$ at the local radiation time t as:

$$P(t) = \frac{2e^2}{3m^2c^3}(\frac{d\vec{p}}{dt})^2, \quad (1)$$

when $\vec{a}_{acce} \| \vec{v}$, and

$$P(t) = \frac{2e^2}{3m^2c^3}(\frac{d\vec{p}}{dt})^2\gamma^2, \quad (2)$$

when $\vec{a}_{acce} \perp \vec{v}$. Here $\vec{p}$ is the electron momentum, γ is the relativistic factor, e and m are the charge and mass of the electron, respectively. So the radiation due to the transverse acceleration is γ^2 stronger than the one due to the longitudinal acceleration. For the synchrotron radiation, the radiation is mainly in the direction of electron motion and concentrated within an angle of θ with $\triangle\theta \sim \frac{1}{\gamma}$.

Based on the above knowledge, in the PIC code we only consider the radiation due to the transverse acceleration and only the electrons whose $\gamma \geq 5$ are assumed to contribute the radiation.

By use of the normalized variables as in the PIC code ($p \sim p/mc, t \sim t/T_0 = \omega_0 t/2\pi$), we can get the momentum variation rate as:

$$\frac{dp_{rad}}{dt} = \frac{2e^2}{3mc^2\lambda_0}(\frac{dp}{dt})^2\gamma^2. \quad (3)$$

In one simulation step it changes:

$$\begin{aligned}(\frac{dp_{rad}}{dt})dt &= (\frac{4}{9}\frac{e^2}{hc/2\pi}dp)\times(\frac{3\gamma^2}{4\pi}\frac{dp}{dt})\times\frac{h\omega_0/2\pi}{mc^2} \\ &= n_{ph}\frac{\omega_c}{\omega_0}\frac{E_{ph0}(eV)}{5.11\times10^5},\end{aligned}$$

where h is the Planck constant, ω_0 is the laser frequency and E_{ph0} is the photon energy of the laser pulse. To be simply, in the PIC code we also assume the radiation is in form of photons. The photon frequency is ω_c and the corresponding photon number is $n_{ph} = 8\pi e^2 dp/9hc$. The radiation reaction force on the electron then is:

$$\begin{aligned}\frac{dp_{rad}}{dt} &= \frac{4}{9}\alpha\times\frac{3\gamma^2}{4\pi}\times\frac{E_{ph0}(eV)}{5.11\times10^5}(\frac{dp}{dt})^2 \\ &= 1.8791\times10^{-9}\gamma^2(\frac{dp}{dt})^2/\lambda_0(\mu m).\end{aligned}$$

The reaction force points to the opposite direction of the electron motion. On the other hand, the electron also feels the external force as (Here we only show the transverse force due to laser field.):

$$\frac{dp_{Laser\perp}}{dt} = 2\pi q_e(\vec{E} + \vec{\beta}\times\vec{B})_\perp = -2\pi(\vec{E}_\perp + \vec{\beta_x}\times\vec{B}_\perp), \quad (4)$$

where E and B are the intensities of electric and magnetic fields normalized by $m\omega_0 c/e$. We can get the threshold of the laser intensity for the obvious radiation damping effect by using:

$$\frac{dp_{rad}}{dt} \sim \frac{dp_{Laser\perp}}{dt}. \quad (5)$$

It is:

$$1.181\times10^{-8}\gamma^2(\vec{E} + \vec{\beta_x}\times\vec{B})/\lambda_0(\mu m) \sim 1. \quad (6)$$

Usually in a laser pulse, $|\vec{E}| = |\vec{B}| = a$. For an electron moving along with a linearly polarized laser pulse, we have:

$$\begin{aligned}p_y &= a \\ p_x &= a^2/2 > 0 \\ \gamma &= 1 + a^2/2\end{aligned}$$

Here a is the normalized laser field. To get an obvious radiation effect, it should satisfy $\gamma a \geq 8.47\times10^7$, correspondingly the laser intensity should satisfy: $a \geq 550$. It is about 4.2×10^{23} W/cm^2 for a laser with a wavelength of 1 μm, which is higher than the current running laser system. However, for an electron with longitudinal velocity of $\beta_x \simeq 0$, Eq. (6) changes to $\gamma^2 a \geq 8.47\times10^7$. When the electron moves in the opposite direction of the laser pulse with the longitudinal velocity $\beta_x \simeq -1$, then one can get $\gamma^2 a \geq 4.23\times10^7$. That is the threshold of a can be γ times smaller when the electrons with the same energy (γ) move backward (see Fig. 1). The reason is that the radiation force is proportion to the square of the acceleration force. For the electrons moving forwards the transverse force they feel is about zero ($\vec{E} + \vec{\beta_x}\times\vec{B} \approx 0$), so the radiation force is even smaller. However, for the electrons moving backwards, the felt transverse acceleration force is about $4\pi q_e\vec{E}$, so the radiation force is much larger.

SIMULATION RESULTS AND DISCUSSION

In the following, we use PIC simulations to check the radiation reaction effects and show their importance on ion acceleration. To simulate the damping effects we suppose that, at any given moment of time, the electron radiation spectrum is synchrotron like [11]. The critical frequency ω_c is given by the relation $\omega_c = (3/4\pi)\gamma^2|\triangle P_\perp|/(dt)$; $\triangle P_\perp$ is the variation of transverse electron momentum force during the time step of dt. In our PIC code, we follow trajectories of each electron and calculate the emission during the interaction. We calculate the damping effects by considering the electron's recoil due to the emitted radiation. The recoil force is included in the equations of electron motion. We should mention that our method is different with the one used by Martins *et al.* in OSIRIS code, in which they can get the radiation field and frequency in a faraway virtual detector [12]. In our code we do not pay attention to the received radiation field on the virtual detector. Our main attention is focused on the reaction effects on plasma itself. The radiation we recorded every simulation step is the photons radiated in the local time of radiation, not the one at the observation time. Our method is also simpler than the one used by Sokolov *et al.*, in

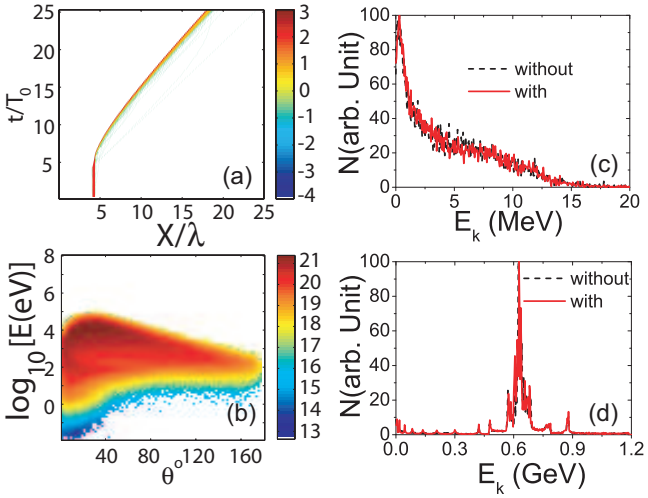

Figure 2: (color online) (a) Spatial-temporal distribution of the electron density. (b) Electron energy spectra in the simulations with and without radiation damping effects at $t = 20\ T_0$. (c) The energy angular distribution of the radiated photons during $t = 20\ T_0$ and $t = 21\ T_0$. The colorbar shows the relative photon number in the logarithmic value. (d) Proton spectra in the simulations with and without radiation damping effects at $t = 20\ T_0$. Here $a = 100$ and $n = 100$.

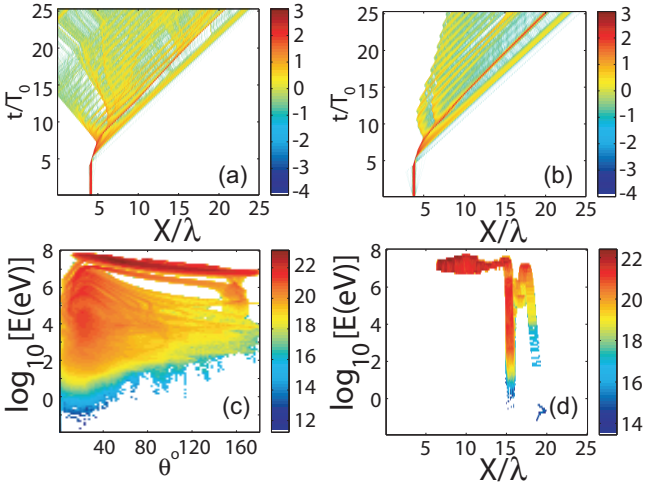

Figure 3: (color online) (a) Spatial-temporal distribution of the electron density for the simulation without radiation damping effects. (b) The case with radiation damping effect. (c) The energy angular distribution of the radiated photons during $t = 20\ T_0$ and $t = 21\ T_0$. The colorbar shows the relative photon number in the logarithmic value. (d) The radiated photon energy and positions during $t = 20\ T_0$ and $t = 21\ T_0$. The colorbar shows the relative photon number in the logarithmic value. Here $a = 180$ and $n = 100$.

which the modified non-perturbative Lorentz-Abraham-Dirac equation is resolved for particle motion instead of the normal Lorentz equation [13]. Although with our method the code cannot gives a correct radiation field on a virtual detector, it is relatively simple and can give appropriate description for the plasmas under radiation damping. Our findings are similar with Naumova *et al.* as they study the hole boring process for fast ignition, however, our main interest is on the ion acceleration in the laser foil interaction.

We take 1D-PIC simulations with the KLAP-1D code [14]. In the simulation, the laser pulse has trapezoidal temporal intensity profile ("linear increase-plateau-linear decrease") with the pulse length $1\lambda/c$-$16\lambda/c$-$1\lambda/c$. Here $\lambda = 1\ \mu m$ is the laser wavelength. The normalized laser electric field $a = eE/m\omega_0 c$ changing from 100 to 500 are used. The target plasma are composed of electrons and protons and they are initially uniformly distributed from $x = 4\ \lambda$ to $x = 4.3\ \lambda$. The plasma density is fixed to be $100\ n_c$ with the critical density $n_c = 1.1{\times}10^{21}/cm^3$.

For the presently fixed plasma density we find when the laser intensity is lower than $a{\sim}125$ the radiation effects on the particle energy spectrum is not observable. Fig. 2(a) shows the spatial temporal distribution of the electron density in the simulation of $a = 100$. In this condition, the ions are accelerated in the radiation pressure dominated region. Electrons and ions are moving together and the acceleration is phase stable. No obvious electron backward motion happens. The electron energy spectrum does not vary so much between the two simulations with and without radiation damping as shown in Fig. 2(c). There is a sharp peak in the proton spectrum with the position at 0.63 GeV after 16 T_0 acceleration time which is close to the theoretical value of 0.66 GeV. Fig. 2(c) shows the energy angular distribution of the radiated photons. Most of the radiation is in the forward direction and the photon energies are about 10 KeV. From the simulation we calculate the average radiation power is about $1.64 \times 10^{17}\ W/cm^2$ which is negligible compared to the laser power of $2.76 \times 10^{22}\ W/cm^2$.

When we increase the laser intensity further to $a = 180$, the radiation damping effects obviously appears. Fig. 3(a,b) show the spatial temporal distribution of the electron density in the two compared simulations (with and without radiation effects). As we see when there is no radiation effects amount of electrons move backwards and the electron density distribution disperses in space. On the contrary, after considering the radiation effects this kind of backward acceleration has been suppressed. More electrons are concentrated and move along with the ion bunch as shown in Fig. 3(b). We show the energy angular distribution of the radiated photons in Fig. 3(c). It composes of two parts. Except the lower part with low photon energy which is similar with the one in Fig. 2(c) (We call this "low energy radiation".), there is a high energy part whose radiation direction is uniformly distributed in the forward and backward directions (We call this "high energy radiation"). To find the source electrons for these radiated photons, we show the radiation position distri-

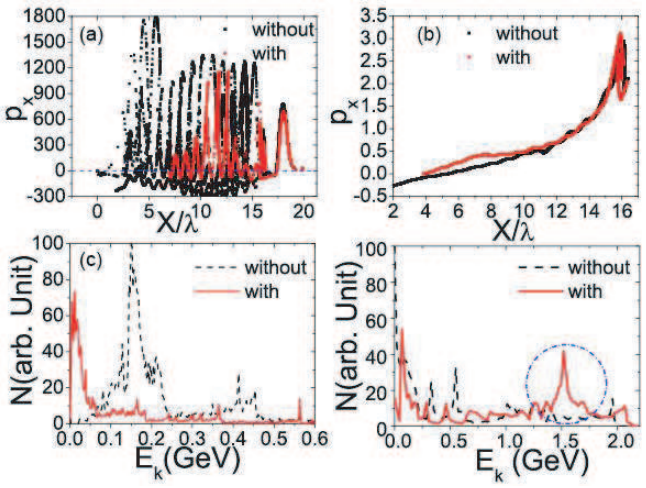

Figure 4: (color online) (a) Electron distribution in the $x-p_x$ phase space, the momentum is normalized by $m_e c$; (b) Proton distribution in the $x-p_x$ phase space; (c) Electron energy spectrum, the momentum is normalized by $m_i c$; (d) Proton energy spectrum. The time here is $t = 20\ T_0$.

bution in Fig. 3(d). Comparing with the positions of the electrons at $t = 20\ T_0$ in Fig. 3(b), we can see the low energy radiation ($E_{photon} < 1\ MeV$) mainly comes from the electrons moving with the ion bunch and the radiation mainly concentrates within the angle of 20^o, the high energy photons (E_{photon}~22.5 MeV) are radiated by the electrons which move behind the ion bunch where the plasma is transparent to the laser pulse and electrons move both forwards and backwards, the radiation is also almost uniformly in the angular distribution. The total radiation power density is about $8.84 \times 10^{21}\ W/cm^2$ which is almost 10% of the laser power density.

Particle distributions in the phase space are shown in Fig. 4(a,b). Electrons have much smaller volume in the phase space when the radiation damping is included in the simulation. In this case no backward ion acceleration has been found. Much more ions are confined in the front accelerating bunch compared with the simulation without radiation damping. The electron energy spectrum also shows that electrons have a much lower peak energy (10 MeV) in the radiation included simulation, however, it is about 150 MeV in the simulation without radiation damping. Proton energy spectrum shown in Fig. 4 confirms much more protons are concentrated and accelerated in the bunch whose peak energy is about 1.5GeV at $t = 20\ T_0$.

From the energy point of view, at $t = 20\ T_0$, totally $5.01 \times 10^9\ J/cm^2$ laser energy density has been transported into the simulation box. When no radiation damping is included, among them 2.44% ($1.22 \times 10^8\ J/cm^2$) transforms to electrons and 6.93% ($3.47 \times 10^8\ J/cm^2$) transforms to protons. When radiation damping is included, 1.23% ($6.15 \times 10^7\ J/cm^2$) transforms to electrons and 11.16% ($5.59 \times 10^8\ J/cm^2$) transforms to protons. As we see radiation damping reduces the electron energy, however, it improves the proton acceleration. Neglect of radiation damping gives a lower estimation of energy conversion efficiency and worse spectrum.

In our simulations, we find that the high energy radiation appears when $a > 125$. Its quotient among the total radiation increases with the laser intensity. When $a > 300$, there is only high energy radiation. These different radiation profiles also reflect the different acceleration scenarios. From the balance between the forces due to electrostatic field and radiation pressure [8]:

$$\pi n_0^2 l^2 = \frac{a_0^2}{\pi} \frac{1-\beta_e}{1+\beta_e}, \tag{7}$$

where l is the thickness of the target normalized by laser wave length (λ_0) and $\beta_e = a/(a + \sqrt{m_i n_0})$ is the relativistic hole boring velocity [15], we can get the critical laser intensity for the laser pulse transmitting through the target. For our present simulation parameters: $n_0 = 100, l = 0.3, m_i = 1836$, we get $a_{cr} \approx 117$. The intensity is close to the critical value ($a \approx 125$) for the high energy radiation. It means when the laser intensity is higher than a_{cr}, the target tends to be transparent to the laser pulse. Stable (at least in the 1D case) structure of radiation dominated ion acceleration begins mixing with other acceleration mechanism (such as BOA). However, some ions can still be accelerated by the radiation pressure. The amount of these ions depends on the laser intensity. Other ions are accelerated or decelerated by the dispersed electrons. When the laser intensity increases further, radiation pressure acceleration disappears completely. Ions can only be accelerated in the heated electron pool which moves with the laser pulse. In this scenario, the radiation damping is important and necessary, which actually makes the electron pool cooling down and improves the ion acceleration. Further investigation still needs for this kind of acceleration scenario.

SUMMARY AND DISCUSSION

In summary, by use of PIC simulations we studied the radiation reaction effects on the ion acceleration in the radiation pressure dominated region and the transparent plasma region. We find radiation damping effects are important for the electrons moving backwards and immersed in the laser pulse. Self-radiation impedes backward motion, cools down the electrons and makes more ions be concentrated and accelerated. We notice recently many studies on ion acceleration by use of ultrathin foil target, in which target plasma is almost transparent to the laser pulse. Electrons are dancing with the transmitted relatively long laser pulse. The local charge separation field takes in charge of ion acceleration. In this

condition, a correct electron distribution in phase space is important to get the correct final maximum accelerated ion energy and acceleration scaling. When the laser intensity is larger than $a = 100$, radiation reaction could change the electron distribution in phase space. Furthermore, with future laser system such as ELI ($a > 1000$), laser intensity is high enough to awake the contribution of radiation damping. Even for the electrons move forward, the radiation reaction should be considered. It deserves and is necessary to include the radiation reaction effects in the future PIC simulations when ultra intense laser pulse is used.

ACKNOWLEDGEMENTS

This work is supported by the DFG programs TR18 and GRK1203. MC acknowledges support by the Alexander von Humboldt Foundation. ZMS is supported in part by the National Nature Science Foundation of China (Grants No. 10674175, 10734130) and the National Basic Research Program of China (Grant No. 2007CB815100).

References

[1] For detailed information on ELI system, see the website: http://www.extreme-light-infrastructure.eu/eli-home.php.

[2] Caldwell A, Lotov K, Pukhov A, and Simon F 2009 *Nature Phys.* **5** 363; Geddes C G R, Nakamura K, Plateau G R *et al* 2008 *Phys. Rev. Lett.* **100** 215004; Esarey E, Schroeder C B, and Leemans W P 2009 *Rev. Mod. Phys.* **81** 1229

[3] Macchi A *et al* 2005 *Phys. Rev. Lett.* **94** 165003; Fuchs J *et al* 2006 *Nature Phys.* **2** 48; Hegelich B M *et al* 2006 *Nature* **439** 441; Macchi A, Veghini S, Pegoraro F 2009 *Phys. Rev. Lett.* **103** 085003; Tripathi V K *et al* 2009 *Plasmas Phys. Control. Fusion* **51** 024014

[4] Thaury C, Quere F, Geindre J P *et al* 2007 *Nature Phys.* **3** 424

[5] Henig A, Kiefer D, Markey K, *et al* 2009 *Phys. Rev. Lett.* **103** 045002

[6] Pukhov A 2001 *Phys. Rev. Lett.* **86** 3562; Hegelich B M *et al* 2002 *Phys. Rev. Lett.* **89** 085002; Esirkepov T *et al* 2002 *Phys. Rev. Lett.* **89** 175003

[7] Esirkepov T *et al* 2004 *Phys. Rev. Lett.* **92** 175003; Robinson A P L, *et al* 2008 *New J. Phys.* **10** 013021

[8] Chen M, Pukhov A, Yu T P, and Sheng Z M 2009 *Phys. Rev. Lett.* **103** 024801

[9] Lin Y *et al* 2007 *Phys. Plasmas* **14** 056706

[10] Naumova N *et al* 2009 *Phys. Rev. Lett.* **102** 025002

[11] Kiselev S *et al* 2004 *Phys. Rev. Lett.* **93** 135004

[12] Martins J L, Martins S F, Fonseca R A, and Silva L O 2009 *Proc. of SPIE* **7359** 73590V-1

[13] Sokolov I V, Naumova N M, Nees J A *et al* 2009 *arXiv:0904.0405v1*

[14] Chen M, Sheng Z M, Zheng J, Ma Y Y, and Zhang J 2008 *Chinese J. Comput. Phys.* **25** 0043; Chen M, Sheng Z M, Ma Y Y, and Zhang J 2006 *J. Appl. Phys.* **99** 056109

[15] Robinson A P L *et al* 2009 *Plasma Phys. Control. Fusion* **51** 024004